Thermal and Quantum Melting Phase Diagrams for a Magnetic-Field-Induced Wigner Solid

Meng K. Ma,[1] K. A. Villegas Rosales,[1] H. Deng,[1] Y. J. Chung,[1] L. N. Pfeiffer,[1] K. W. West,[1] K. W. Baldwin,[1] R. Winkler,[2] and M. Shayegan[1]

[1]*Department of Electrical Engineering, Princeton University, Princeton, New Jersey 08544, USA*
[2]*Department of Physics, Northern Illinois University, DeKalb, Illinois 60115, USA*

(Received 6 January 2020; accepted 12 June 2020; published 14 July 2020)

A sufficiently large perpendicular magnetic field quenches the kinetic (Fermi) energy of an interacting two-dimensional (2D) system of fermions, making them susceptible to the formation of a Wigner solid (WS) phase in which the charged carriers organize themselves in a periodic array in order to minimize their Coulomb repulsion energy. In low-disorder 2D electron systems confined to modulation-doped GaAs heterostructures, signatures of a magnetic-field-induced WS appear at low temperatures and very small Landau level filling factors ($\nu \simeq 1/5$). In dilute GaAs 2D hole systems, on the other hand, thanks to the larger hole effective mass and the ensuing Landau level mixing, the WS forms at relatively higher fillings ($\nu \simeq 1/3$). Here we report our measurements of the fundamental temperature vs filling phase diagram for the 2D holes' WS-liquid thermal melting. Moreover, via changing the 2D hole density, we also probe their Landau level mixing vs filling WS-liquid quantum melting phase diagram. We find our data to be in good agreement with the results of very recent calculations, although intriguing subtleties remain.

DOI: 10.1103/PhysRevLett.125.036601

The Wigner solid (WS), an ordered array of electrons, favored when the Coulomb repulsion energy dominates over the thermal and Fermi energies, is one of the longest-anticipated and most exotic correlated phases of a strongly interacting electron system [1]. In a low-disorder, two-dimensional electron system (2DES) under a large perpendicular magnetic field (B), the Fermi energy is quenched and the electrons condense into the lowest Landau level (LL). If the separation between the LLs is large compared to the Coulomb energy so that LL mixing (LLM) can be ignored, a magnetic-field-induced, 2D quantum WS is expected at very small LL filling factors ($\nu \lesssim 1/5$) [2–5]. There is, however, a close competition with interacting liquid phases, such as the fractional quantum Hall states (FQHSs) [6]. In very high mobility 2DESs confined to GaAs quantum wells where LLM is small, insulating phases are seen near the FQHS at $\nu = 1/5$, and are generally believed to signal the formation of a WS, pinned by the small but ubiquitous disorder [7–24]. Many properties of these insulating phases support the pinned WS picture [17]; these include the nonlinear current-voltage and noise characteristics [10–13], microwave resonances [7,11,19,20], photoluminescence [15,16], nuclear magnetic resonance features [21], tunneling resonances [23], and screening characteristics [24]. There is also a recent experiment in a GaAs bilayer electron system with very imbalanced densities where one layer is near $\nu = 1/2$ and contains composite fermions while the other layer is at very low fillings ($\nu \ll 1/5$) and hosts a WS [22]. The commensurability oscillations of the composite fermions induced by the periodic potential of the WS layer are used to directly probe the lattice constant of the WS.

The 2D hole systems (2DHSs) in low-disorder GaAs quantum wells provide a particularly exciting platform for studies of the quantum WS phases, both at $B = 0$ [25–27] and at high B [23,27–37]. The effective mass for holes in GaAs is $m^* \simeq 0.5$ (in units of the free electron mass) [38], much larger than $m^* \simeq 0.067$ for GaAs 2D electrons, rendering the 2DHS effectively more dilute and therefore more interacting; note that the r_s parameter, the interparticle distance in units of the effective Bohr radius, scales with m^*. Signatures of a quantum WS at $B = 0$ have indeed been reported in dilute GaAs 2DHSs with very large r_s [25–27]. At high B, the larger m^* means that the LL separation is small so that there is a significant mixing of the higher LLs into the collective states of the 2D system. (For our samples reported here, the LLM parameter κ, defined as the ratio of the Coulomb to cyclotron energies, ranges between ~5 and 16.) Such LLM generally weakens the FQHSs, whose stability relies on short-range correlations, and favors the ground states with long-range order, such as the WS [39–45]. Consistent with this expectation, experiments on GaAs 2DHSs have indeed shown that the onset of the magnetic-field-induced WS moves to higher fillings ($\nu \simeq 1/3$, compared to $\nu \simeq 1/5$ for 2D electrons) [17,28–37]. A recent study on ZnO 2DESs with parameters similar to GaAs 2DHSs also shows the onset of the WS at $\nu \simeq 1/3$ [46]. Here we present experiments on very low

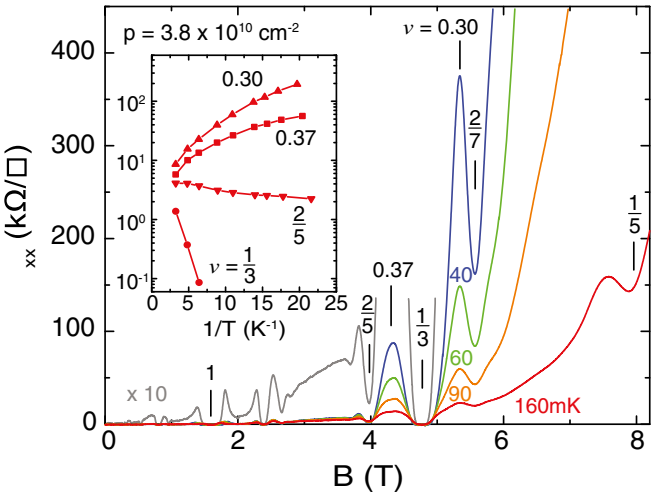

FIG. 1. Temperature dependence of the longitudinal resistivity ρ_{xx} vs magnetic field B at $p = 3.8$. The y scale for the grey trace is expanded by a factor of 10. The inset shows the Arrhenius plots of ρ_{xx} at $\nu = 0.30$, 0.37, 2/5, and 1/3.

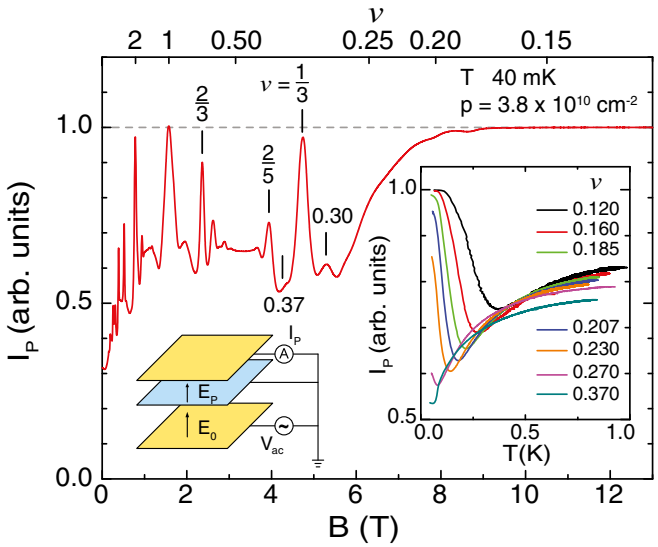

FIG. 2. Left inset: Schematic of the measurement setup. Top and bottom yellow plates represent front and back gates and the middle blue plate the 2DHS layer. An ac excitation voltage V_{ac} is applied to the bottom gate which generates an electric field E_0, and subsequently a penetrating electric field E_P as a function of the screening efficiency of the 2DHS. A current I_P in response to E_P is then measured. Trace in the main figure shows I_P, normalized to its maximum value, vs B. Horizontal line marks the maximum of I_P when the 2DHS screening is minimum. Right inset: I_P vs temperature traces for ν ranging from 0.120 to 0.370.

disorder 2DHSs confined to modulation-doped GaAs quantum wells, and probe two fundamental WS-liquid phase diagrams: a temperature vs ν phase diagram for the thermal melting of the WS, and a κ vs ν diagram for its quantum melting.

We studied 2DHSs confined to modulation-doped, 30-nm-wide GaAs quantum wells (QWs) grown on GaAs (100) substrates. The details of the sample parameters are provided in the Supplemental Material (SM) [47]. The samples have 2DHS densities (p) ranging from 2.0 to 7.9, in units of 10^{10} cm^{-2} which we will use throughout this Letter, and their low-temperature mobility is $\simeq 1.5 \times 10^6$ cm^2/Vs. We present data in the main text for two samples with densities $p = 3.8$ and 7.9; data for other densities are shown in the SM [47]. We performed all our measurements on 4 mm × 4 mm van der Pauw geometry samples, which are fitted with gate electrodes deposited on their top and bottom surfaces. The density in a given sample is tuned using both the front and back gates while keeping the charge distribution in the QW symmetric. We made measurements primarily in a dilution refrigerator with a base temperature of $\simeq$40 mK.

Figure 1 shows the temperature dependence of longitudinal resistivity ρ_{xx} vs B at $p = 3.8$. The expanded (grey) trace at $\simeq$40 mK shows a series of FQHSs attesting to the good quality of the sample. At the highest temperature, there is even a hint of a developing $\nu = 1/5$ FQHS. The $\nu = 1/3$ FQHS is fully developed and has a vanishing ρ_{xx} minimum at the lowest temperatures. On the other hand, on its flanks (e.g., at $\nu = 0.30$ and 0.37), ρ_{xx} has very high values, which decrease rapidly as the temperature is raised. This insulating behavior is generally believed to signal a disorder-pinned WS state [17,28,29,31–37], and can be seen more conveniently in the Arrhenius plot shown in the Fig. 1 inset. Also shown in this inset are the temperature dependences of ρ_{xx} at $\nu = 2/5$ and 1/3. In contrast to the insulating behavior at $\nu = 0.30$ and 0.37, ρ_{xx} at $\nu = 1/3$ and 2/5 decreases as the temperature is lowered, and is activated at $\nu = 1/3$ with an energy gap of $\simeq$1.8 K.

We probe the thermal melting of the WS by monitoring the screening efficiency [24,54–56] of the 2DHS. This technique was used recently [24] to study the magnetic-field-induced WS in GaAs 2DESs near $\nu \simeq 1/5$, and the deduced melting phase diagram was found to be in good agreement with previous measurements. The measurement setup is shown schematically in the Fig. 2 inset. The top and bottom yellow plates represent the front and back gates. The blue layer in the middle represents the 2DHS we are probing. We apply an ac excitation voltage V_{ac} of 1 mV between the back and front gates at 22 kHz as shown in the inset. This ac voltage generates an electric field E_P penetrating through the 2DHS. The magnitude of E_P depends on the screening efficiency of the 2DHS. The magnitude of the penetrating current I_P is then probed in response to E_P.

The trace in Fig. 2 shows I_P vs B at our base temperature ($\simeq$40 mK) and $p = 3.8$. At fillings where the 2DHS is in an integer or FQHS, its bulk is incompressible and the screening is minimal. As a result, I_P shows a maximum. When the bulk is compressible between the QHSs, I_P comes down as a result of the increasing screening efficiency of the 2DHS. At $\nu = 0.30$, where the WS phase develops, I_P shows a local maximum, consistent with the WS phase being insulating

and having, therefore, lower screening efficiency. I_P at $\nu = 0.37$ shows a "shoulder" at this density, but develops into a well-defined local maximum at lower densities [47]. At very high B, beyond $\simeq 8$ T, the 2DHS becomes strongly insulating and I_P approaches the same value it has at the strongest QHSs, consistent with the screening efficiency being minimal.

The right inset in Fig. 2 shows the temperature dependence of I_P at different ν. At $\nu = 0.120$, I_P starts with a high value at the lowest temperature, consistent with an insulating WS. At the highest temperatures, where we expect the WS to have melted, I_P saturates at a value which is lower than its maximum value. This is consistent with a compressible liquid phase which has a higher screening efficiency than the WS. However, as the temperature is raised, instead of decreasing monotonically from its low-temperature value and saturating at the high-temperature limit, I_P shows a well-defined minimum at a critical temperature T_C. This temperature dependence is generic for all the traces shown in the Fig. 1 inset except for $\nu = 0.370$ and $\nu = 0.270$, where I_P at the lowest temperature is lower than its high-temperature limit. This is because the lowest temperature achieved in our measurements ($T \simeq 40$ mK) is close to T_C for these two fillings; we expect I_P to increase if lower temperatures were accessible.

The data shown in the Fig. 2 inset suggest that the 2DHS becomes particularly efficient at screening near T_C. A qualitatively similar behavior was recently seen in low-density GaAs 2D electron systems [24]. Associating T_C with the melting temperature of the WS, Ref. [24] found the measured dependence of T_C on ν to be consistent with the WS melting phase diagrams reported previously for the magnetic-field-induced WS in GaAs 2DESs. It is not clear why a WS should become particularly efficient at screening as it melts. It is possible that the minimum in I_P signals the presence of an intermediate phase near the melting temperature, as has been suggested in a recent report [37]. Alternatively, very recent calculations [57] suggest that dissipation from mobile dislocations and uncondensed charge carriers become especially important near the melting of the WS phase. It is possible that they contribute to the extra screening at the melting.

Associating T_C with the melting temperature of the WS, a plot of our measured T_C vs ν, as shown in Fig. 3, provides the WS thermal melting phase diagram of a 2DHS at $p = 3.8$. As ν increases from small values, T_C decreases until the WS phase is "interrupted" by the well-developed $\nu = 1/3$ FQHS. When ν is higher than $1/3$, there is a reentrant WS phase between the $1/3$ and $2/5$ FQHSs, around $\nu \simeq 0.37$. We note that our $T_C \simeq 50$ mK at $\nu = 0.37$ is consistent with the WS melting temperature reported in Ref. [37] for a 2DHS with a similar density at $\nu = 0.375$.

The competition between the WS and FQHS liquid phases depends on the mixing between the LLs [28–37,39–45]. This is often quantified in terms of the LLM parameter κ, defined as the ratio between the Coulomb energy and the

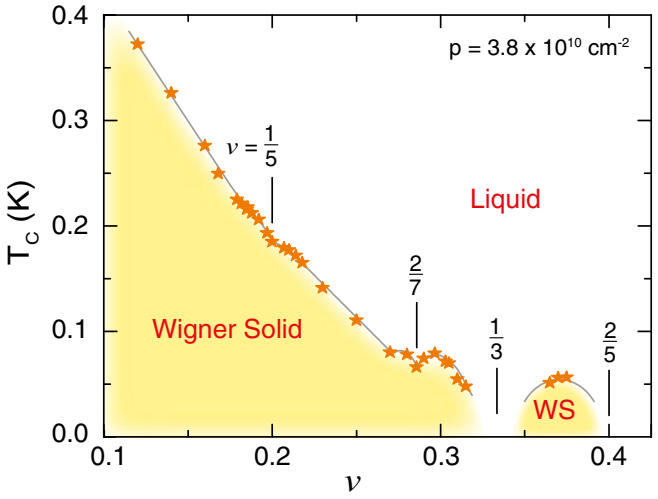

FIG. 3. WS thermal melting phase diagram. The yellow and white regions indicate the solid and liquid phases, respectively. The grey line connecting the measured data points is a guide to the eye.

LL separation: $\kappa = (e^2/4\pi\epsilon_0\epsilon l_B)/(\hbar eB/m^*)$, where $l_B = \sqrt{\hbar/eB}$ is the magnetic length. Note that $\kappa \propto m^*$. When κ is large, the mixing with the higher LLs reduces the FQHS energy gaps and favors the formation of a WS at filling factors higher than $1/5$ [28–37,39–45]. Recent theoretical work by Zhao *et al.* [45] directly mapped out a zero-temperature phase diagram for the quantum melting of

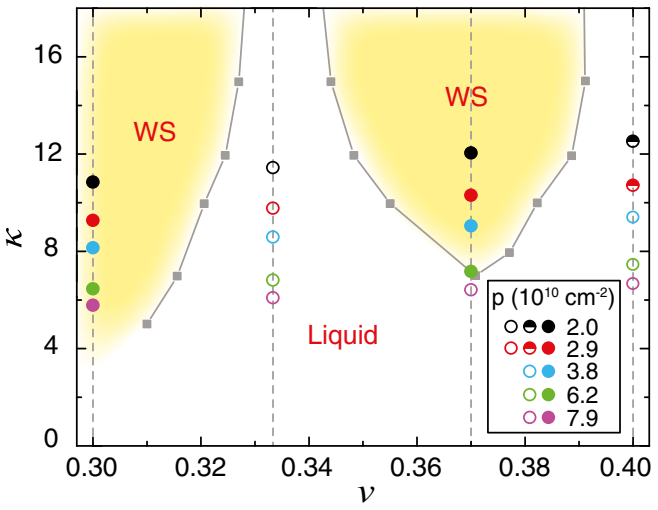

FIG. 4. WS quantum melting phase diagram, with the Landau level mixing parameter κ and ν for the axes. The grey solid squares connected by the guide-to-the-eye lines are from theoretical calculations [45]. The yellow and white regions indicate the predicted WS and liquid phases. The color-coded circles represent experimental data points deduced from measurements at six different densities, as listed in the inset box. The closed and open circles indicate WS and liquid phases, respectively. The half-filled circles are used to imply a close competition between the WS and the liquid phase.

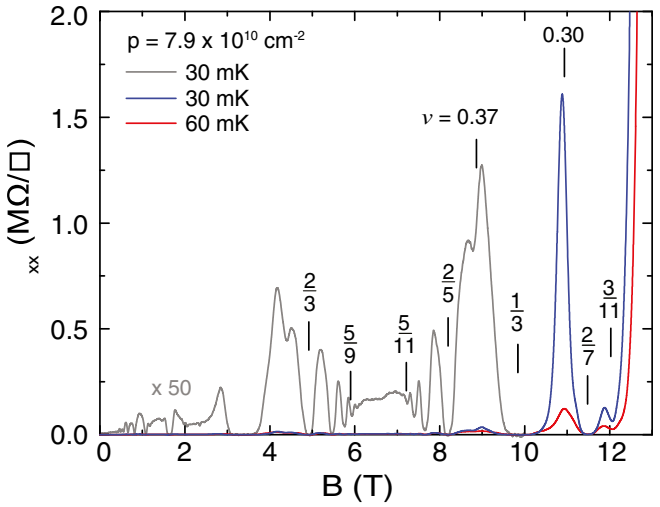

FIG. 5. Magnetoresistivity data for a 2DHS with $p = 7.9$ at 30 and 60 mK. The y scale for the grey trace is expanded by a factor of 50 to show the numerous observed FQHSs, attesting to the high quality of the 2DHS.

the WS in the κ-ν space. The calculated phase diagram is reproduced in Fig. 4 for a direct comparison with our experimental results.

Our GaAs 2DHSs allow us to test the role of LLM. Compared to the GaAs 2DES, the 2DHSs have large m^*. Because of the nonparabolicity of the valence bands and spin-orbit coupling, however, m^* for 2DHS is intrinsically complex and depends on the specific sample parameters such as the QW width and the symmetry of the charge distribution [58]. For a systematic study, it is therefore essential to use both the front and back gates to keep the hole charge distribution in the QW symmetric while changing the density. Cyclotron resonance experiments [38] on 2DHSs confined to symmetric, 30-nm-wide QWs grown on GaAs (100) substrates yield a weakly density-dependent $m^* \simeq 0.48$ in the density range we studied here. We use this value of m^* to determine values of κ at a set of representative filling factors $\nu = 0.30$, $1/3$, 0.37, and $2/5$ for our samples, and show these in Fig. 4 using symbols described in the inset.

For $p = 3.8$, the experimental data are represented by blue circles in Fig. 4. Data at all four fillings are consistent with the calculation results: as ν decreases, the 2DHS ground state changes from a FQHS at $\nu = 2/5$ to a WS at 0.37, then to a FQHS at $1/3$, and finally back to a WS at 0.30. In order to lower κ, we made measurements on a higher density 2DHS. The ρ_{xx} vs B data for this sample are shown in Fig. 5. At this density, well-developed FQHSs are seen at $\nu = 1/3$, $2/5$, and $2/7$. Moreover, in contrast to the trace at $p = 3.8$ (Fig. 1), ρ_{xx} at $\nu = 0.37$ has comparable value to ρ_{xx} at higher fillings, and depends only very weekly on temperature. This implies that the ground state at $\nu = 0.37$ is not a WS at $p = 7.9$. On the other hand, similar to the data for $p = 3.8$, the trace in Fig. 5 shows a very large and strongly temperature dependent ρ_{xx} peak at $\nu = 0.30$, consistent with a pinned WS. We show the four experimental points for $p = 7.9$ at $\nu = 0.30$, $1/3$, 0.37, and $2/5$, in Fig. 4 by purple circles. The data are again consistent with the theoretical phase diagram: as κ is reduced, the WS phase at $\nu = 0.37$ disappears but it is still present at $\nu = 0.30$.

We also performed measurements at three other densities, $p = 6.2$, 2.9, and 2.0; the results are presented in the SM [47], and are summarized in Fig. 4. For $p = 6.2$, the results are consistent with the theoretical phase diagram. For the lowest two densities, $p = 2.9$ and 2.0, however, there is a hint of a FQHS at $\nu = 2/5$, but the data suggest a competition with an insulating phase, signaled by a rise in ρ_{xx} as the temperature is lowered. This might indicate an apparent discrepancy between the experimental data and the theoretical phase diagram, which predicts that the ground state should be a FQHS (liquid) phase at $\nu = 2/5$ in the entire range of κ in Fig. 4. We believe that disorder, whose role certainly increases at very low densities but is neglected in the theory of Ref. [45], is at least partly responsible for the discrepancy [47]. It is worth remembering that, in early studies of GaAs 2DES, qualitatively similar observations were made. Early samples, which had lower quality, showed a competition between a FQHS and an insulating phase at $\nu = 1/5$ [8], and a clear FQHS with a vanishing ρ_{xx} at the lowest temperature was only seen when samples of much better quality were available [9].

In conclusion, we report a thermal melting phase diagram for the magnetic-field-induced WS in GaAs 2DHSs deduced from its screening efficiency. The phase diagram shows the clear reentrant behavior of the WS around the FQHS at $\nu = 1/3$, and provides data for a quantitative comparison with future theoretical calculations. We also systematically study the quantum melting of the WS as a function of LM, varied by changing the 2DHS density. While we find good overall agreement with the results of calculations, we would like to emphasize the complexity of the 2DHS LL diagram [58]. As discussed in more detail in the SM [47], the 2DHS LLs are nonlinear and also can cross as a function of magnetic field. Moreover, the interaction between holes is subtle because of the multicomponent and mixed (spin and orbital) nature of the hole states. These make a quantitative assessment of the role of LLM challenging. We hope that our experimental data provide incentive for a more precise theoretical evaluation of the role of LLM, as well as disorder, in the competition between the WS and FQHS phases in GaAs 2DHSs.

We acknowledge support by the DOE BES (No. DE-FG02-00-ER45841) Grant for measurements, and the NSF (Grants No. DMR 1709076, No. MRSEC DMR 1420541, and No. ECCS 1906253), and the Gordon and Betty Moore Foundation's EPiQS Initiative (Grant No. GBMF9615) for sample fabrication and characterization. M. S. also acknowledges a QuantEmX travel grant from Institute

for Complex Adaptive Matter and the Gordon and Betty Moore Foundation through Grant No. GBMF5305. We thank J. K. Jain and L. W. Engel for illuminating discussions.

[1] E. Wigner, On the interaction of electrons in metals, Phys. Rev. **46**, 1002 (1934).
[2] Y. E. Lozovik and V. I. Yudson, Crystallization of a two-dimensional electron gas in a magnetic field, JETP Lett. **22**, 11 (1975).
[3] P. K. Lam and S. M. Girvin, Liquid-solid transition and the fractional quantum-Hall effect, Phys. Rev. B **30**, 473(R) (1984).
[4] D. Levesque, J. J. Weis, and A. H. MacDonald, Crystallization of the incompressible quantum-fluid state of a two-dimensional electron gas in a strong magnetic field, Phys. Rev. B **30**, 1056(R) (1984).
[5] A. C. Archer, K. Park, and J. K. Jain, Competing Crystal Phases in the Lowest Landau Level, Phys. Rev. Lett. **111**, 146804 (2013).
[6] D. C. Tsui, H. L. Stormer, and A. C. Gossard, Two-Dimensional Magnetotransport in the Extreme Quantum Limit, Phys. Rev. Lett. **48**, 1559 (1982).
[7] E. Y. Andrei, G. Deville, D. C. Glattli, F. I. B. Williams, E. Paris, and B. Etienne, Observation of a Magnetically Induced Wigner Solid, Phys. Rev. Lett. **60**, 2765 (1988).
[8] R. L. Willett, H. L. Stormer, D. C. Tsui, L. N. Pfeiffer, K. W. West, and K. W. Baldwin, Termination of the series of fractional quantum hall states at small filling factors, Phys. Rev. B **38**, 7881(R) (1988).
[9] H. W. Jiang, R. L. Willett, H. L. Stormer, D. C. Tsui, L. N. Pfeiffer, and K. W. West, Quantum Liquid Versus Electron Solid Around $\nu = 1/5$ Landau-Level Filling, Phys. Rev. Lett. **65**, 633 (1990).
[10] V. J. Goldman, M. Santos, M. Shayegan, and J. E. Cunningham, Evidence for Two-Dimentional Quantum Wigner Crystal, Phys. Rev. Lett. **65**, 2189 (1990).
[11] F. I. B. Williams, P. A. Wright, R. G. Clark, E. Y. Andrei, G. Deville, D. C. Glattli, O. Probst, B. Etienne, C. Dorin, C. T. Foxon, and J. J. Harris, Conduction Threshold and Pinning Frequency of Magnetically Induced Wigner Solid, Phys. Rev. Lett. **66**, 3285 (1991).
[12] Y. P. Li, T. Sajoto, L. W. Engel, D. C. Tsui, and M. Shayegan, Low-Frequency Noise in the Reentrant Insulating Phase Around the 1/5 Fractional Quantum Hall Liquid, Phys. Rev. Lett. **67**, 1630 (1991).
[13] H. W. Jiang, H. L. Stormer, D. C. Tsui, L. N. Pfeiffer, and K. W. West, Magnetotransport studies of the insulating phase around $\nu = 1/5$ Landau-level filling, Phys. Rev. B **44**, 8107 (1991).
[14] M. A. Paalanen, R. L. Willett, R. R. Ruel, P. B. Littlewood, K. W. West, and L. N. Pfeiffer, Electrical conductivity and Wigner crystallization, Phys. Rev. B **45**, 13784(R) (1992).
[15] E. M. Goldys, S. A. Brown, R. B. Dunford, A. G. Davies, R. Newbury, R. G. Clark, P. E. Simmonds, J. J. Harris, and C. T. Foxon, Magneto-optical probe of two-dimensional electron liquid and solid phases, Phys. Rev. B **46**, 7957(R) (1992).
[16] I. V. Kukushkin, N. J. Pulsford, K. v. Klitzing, R. J. Haug, K. Ploog, and V. B. Timofeev, Wigner solid vs incompressible laughlin liquid: Phase diagram derived from time-resolved photoluminescence, Europhys. Lett. **23**, 211 (1993).
[17] For an early review, see M. Shayegan, Case for the magnetic-field-induced two-dimensional Wigner crystal, in *Perspectives in Quantum Hall Effects*, edited by S. D. Sarma and A. Pinczuk (Wiley, New York, 1997), pp. 343–383.
[18] W. Pan, H. L. Stormer, D. C. Tsui, L. N. Pfeiffer, K. W. Baldwin, and K. W. West, Transition from an Electron Solid to the Sequence of Fractional Quantum Hall States at Very Low Landau Level Filling Factor, Phys. Rev. Lett. **88**, 176802 (2002).
[19] P. D. Ye, L. W. Engel, D. C. Tsui, R. M. Lewis, L. N. Pfeiffer, and K. West, Correlation Lengths of the Wigner-Crystal Order in a Two-Dimensional Electron System at High Magnetic Fields, Phys. Rev. Lett. **89**, 176802 (2002).
[20] Y. P. Chen, G. Sambandamurthy, Z. H. Wang, R. M. Lewis, L. W. Engel, D. C. Tsui, P. D. Ye, L. N. Pfeiffer, and K. W. West, Melting of a 2D quantum electron solid in high magnetic field, Nat. Phys. **2**, 452 (2006).
[21] L. Tiemann, T. D. Rhone, N. Shibata, and K. Muraki, NMR profiling of quantum electron solids in high magnetic fields, Nat. Phys. **10**, 648 (2014).
[22] H. Deng, Y. Liu, I. Jo, L. N. Pfeiffer, K. W. West, K. W. Baldwin, and M. Shayegan, Commensurability Oscillations of Composite Fermions Induced by the Periodic Potential of a Wigner Crystal, Phys. Rev. Lett. **117**, 096601 (2016).
[23] J. Jang, B. M. Hunt, L. N. Pfeiffer, K. W. West, and R. C. Ashoori, Sharp tunnelling resonance from the vibrations of an electronic Wigner crystal, Nat. Phys. **13**, 340 (2017).
[24] H. Deng, L. N. Pfeiffer, K. W. West, K. W. Baldwin, L. W. Engel, and M. Shayegan, Probing the Melting of a Two-Dimensional Quantum Wigner Crystal via its Screening Efficiency, Phys. Rev. Lett. **122**, 116601 (2019).
[25] J. Yoon, C. C. Li, D. Shahar, D. C. Tsui, and M. Shayegan, Wigner Crystallization and Metal-Insulator Transition of Two-Dimensional Holes in GaAs at $B = 0$, Phys. Rev. Lett. **82**, 1744 (1999).
[26] M. J. Manfra, E. H. Hwang, S. Das Sarma, L. N. Pfeiffer, K. W. West, and A. M. Sergent, Transport and Percolation in a Low-Density High-Mobility Two-Dimensional Hole System, Phys. Rev. Lett. **99**, 236402 (2007).
[27] R. L. J. Qiu, X. P. A. Gao, L. N. Pfeiffer, and K. W. West, Connecting the Reentrant Insulating Phase and the Zero-Field Metal-Insulator Transition in a 2D Hole System, Phys. Rev. Lett. **108**, 106404 (2012).
[28] M. B. Santos, Y. W. Suen, M. Shayegan, Y. P. Li, L. W. Engel, and D. C. Tsui, Observation of a Reentrant Insulating Phase Near the 1/3 Fractional Quantum Hall Liquid in a Two-Dimensional Hole System, Phys. Rev. Lett. **68**, 1188 (1992).
[29] M. B. Santos, J. Jo, Y. W. Suen, L. W. Engel, and M. Shayegan, Effect of Landau-level mixing on quantum-liquid and solid states of two-dimensional hole systems, Phys. Rev. B **46**, 13639(R) (1992).
[30] V. Bayot, X. Ying, M. B. Santos, and M. Shayegan, Thermopower in the re-entrant insulating phase of a two-dimensional hole system, Europhys. Lett. **25**, 613 (1994).

[31] C.-C. Li, L. W. Engel, D. Shahar, D. C. Tsui, and M. Shayegan, Microwave Conductivity Resonance of Two-Dimensional Hole System, Phys. Rev. Lett. **79**, 1353 (1997).
[32] C.-C. Li, J. Yoon, L. W. Engel, D. Shahar, D. C. Tsui, and M. Shayegan, Microwave resonance and weak pinning in two-dimensional hole systems at high magnetic fields, Phys. Rev. B **61**, 10905 (2000).
[33] G. A. Csáthy, D. C. Tsui, L. N. Pfeiffer, and K. W. West, Possible Observation of Phase Coexistence of the $\nu = 1/3$ Fractional Quantum Hall Liquid and a Solid, Phys. Rev. Lett. **92**, 256804 (2004).
[34] G. A. Csáthy, Hwayong Noh, D. C. Tsui, L. N. Pfeiffer, and K. W. West, Magnetic-Field-Induced Insulating Phases at Large r_s, Phys. Rev. Lett. **94**, 226802 (2005).
[35] W. Pan, G. A. Csáthy, D. C. Tsui, L. N. Pfeiffer, and K. W. West, Transition from a fractional quantum Hall liquid to an electron solid at Landau level filling $\nu = 1/3$ in tilted magnetic fields, Phys. Rev. B **71**, 035302 (2005).
[36] I. Jo, H. Deng, Y. Liu, L. N. Pfeiffer, K. W. West, K. W. Baldwin, and M. Shayegan, Cyclotron Orbits of Composite Fermions in the Fractional Quantum Hall Regime, Phys. Rev. Lett. **120**, 016802 (2018).
[37] T. Knighton, Z. Wu, J. Huang, A. Serafin, J. S. Xia, L. N. Pfeiffer, and K. W. West, Evidence of two-stage melting of Wigner solids, Phys. Rev. B **97**, 085135 (2018).
[38] H. Zhu, K. Lai, D. C. Tsui, S. P. Bayrakci, N. P. Ong, M. Manfra, L. Pfeiffer, and K. West, Density and well width dependences of the effective mass of two-dimensional holes in (100) GaAs quantum wells measured using cyclotron resonance at microwave frequencies, Solid State Commun. **141**, 510 (2007).
[39] D. Yoshioka, Effect of the Landau level mixing on the ground state of two-dimensional electrons, J. Phys. Soc. Jpn. **53**, 3740 (1984).
[40] D. Yoshioka, Excitation energies of the fractional quantum Hall effect, J. Phys. Soc. Jpn. **55**, 885 (1986).
[41] X. Zhu and S. G. Louie, Wigner Crystallization in the Fractional Quantum Hall Regime: A Variational Quantum Monte Carlo Study, Phys. Rev. Lett. **70**, 335 (1993).
[42] R. Price, P. M. Platzman, and S. He, Fractional Quantum Hall Liquid, Wigner Solid Phase Boundary at Finite Density and Magnetic Field, Phys. Rev. Lett. **70**, 339 (1993).
[43] P. M. Platzman and R. Price, Quantum Freezing of the Fractional Quantum Hall Liquid, Phys. Rev. Lett. **70**, 3487 (1993).
[44] G. Ortiz, D. M. Ceperley, and R. M. Martin, New Stochastic Method for Systems with Broken Time-Reversal Symmetry: 2D Fermions in a Magnetic Field, Phys. Rev. Lett. **71**, 2777 (1993).
[45] J. Zhao, Y. Zhang, and J. K. Jain, Crystallization in the Fractional Quantum Hall Regime Induced by Landau-Level Mixing, Phys. Rev. Lett. **121**, 116802 (2018).
[46] D. Maryenko, A. McCollam, J. Falson, Y. Kozuka, J. Bruin, U. Zeitler, and M. Kawasaki, Composite fermion liquid to Wigner solid transition in the lowest Landau level of zinc oxide, Nat. Commun. **9**, 4356 (2018).
[47] See Supplemental Material at http://link.aps.org/supplemental/10.1103/PhysRevLett.125.036601, which includes Refs. [48–53], for more details on sample structure, additional data, and discussions.
[48] T. Ando, A. B. Fowler, and F. Stern, Electronic properties of two-dimensional systems, Rev. Mod. Phys. **54**, 437 (1982).
[49] J. K. Jain, *Composite Fermions* (Cambridge University Press, Cambridge, England, 2007).
[50] T. Kernreiter, M. Governale, R. Winkler, and U. Zülicke, Suppression of Coulomb exchange energy in quasi-two-dimensional hole systems, Phys. Rev. B **88**, 125309 (2013).
[51] L. C. Andreani, A. Pasquarello, and F. Bassani, Hole subbands in strained GaAs-$Ga_{1-x}Al_xAs$ quantum wells: Exact solution of the effective-mass equation, Phys. Rev. B **36**, 5887 (1987).
[52] R. Winkler, E. Tutuc, S. J. Papadakis, S. Melinte, M. Shayegan, D. Wasserman, and S. A. Lyon, Anomalous spin polarization of GaAs two-dimensional hole systems, Phys. Rev. B **72**, 195321 (2005).
[53] M. Tsukada, Two-dimensional crystallization of the electrons in MOS structures induced by strong magnetic field, J. Phys. Soc. Jpn. **42**, 391 (1977).
[54] J. P. Eisenstein, L. N. Pfeiffer, and K. W. West, Negative Compressibility of Interacting Two-Dimensional Electron and Quasiparticle Gases, Phys. Rev. Lett. **68**, 674 (1992).
[55] J. P. Eisenstein, L. N. Pfeiffer, and K. W. West, Compressibility of the two-dimensional electron gas: Measurements of the zero-field exchange energy and fractional quantum Hall gap, Phys. Rev. B **50**, 1760 (1994).
[56] A. A. Zibrov, E. M. Spanton, H. Zhou, C. Kometter, T. Taniguchi, K. Watanabe, and A. F. Young, Even-denominator fractional quantum Hall states at an isospin transition in monolayer graphene, Nat. Phys. **14**, 930 (2018).
[57] L. V. Delacrétaz, B. Goutraux, S. A. Hartnoll, and A. Karlsson, Theory of collective magnetophonon resonance and melting of a field-induced Wigner solid, Phys. Rev. B **100**, 085140 (2019).
[58] R. Winkler, *Spin-Orbit Coupling Effects in Two-Dimensional Electron and Hole Systems*, Springer Tracts in Modern Physics Vol. 191 (Springer-Verlag, Berlin, 2003).